JOURNAL OF GEOPHYSICAL RESEARCH, VOL. 114, E04008, doi:10.1029/2008JE003258, 2009



# Highly charged cloud particles in the atmosphere of Venus

Marykutty Michael,[1] Sachchida Nand Tripathi,[1] W. J. Borucki,[2] and R. C. Whitten[3]

Received 12 September 2008; revised 25 December 2008; accepted 21 January 2009; published 17 April 2009.

[1] The accumulation of charges on cloud particles by the charge transfer of ions and attachment of electrons in the atmosphere of Venus is investigated in the present work. Three cloud layers between 45 and 70 km exist in the atmosphere of Venus. Ions and electrons are produced by the interaction of galactic cosmic rays with the neutral molecules. Ion to particle and electron to particle attachment coefficients are calculated. The charge balance equations include ion-ion recombination, ion-electron recombination, electron attachment to neutrals, electron detachment from negative ions, and attachment of electron and charge transfer from ions to particles. It is found that the ion concentrations are reduced by a maximum of a factor of 5 by charging of the particles, while the earlier studies showed a maximum reduction of about an order of magnitude due to the differences in the surface area of the particles. A similar result is observed in the calculation of electrical conductivity. Both monodisperse and polydisperse distribution of particles are considered. The conductivity was reduced by a factor of 3 when using the monodisperse distribution of particles, while the maximum reduction observed was a factor of 2 when using the polydisperse distribution. This result implies that the monodisperse particle distribution overestimates the effect of particles on the atmospheric conductivity. The ratio of negative to positive charges is found to be very large in the middle and upper cloud layers. The low abundance of the aerosols and high conductivity of the atmosphere appear to rule out lightning activity in the 40 to 70 km altitude region.

**Citation:** Michael, M., S. N. Tripathi, W. J. Borucki, and R. C. Whitten (2009), Highly charged cloud particles in the atmosphere of Venus, *J. Geophys. Res.*, *114*, E04008, doi:10.1029/2008JE003258.

## 1. Introduction

[2] Mariner 10 and Pioneer Venus measurements revealed widespread hazes in the atmosphere of Venus. Generally they cover the entire planet, being most prominent at the bright polar caps [*Taylor et al.*, 1980; *Knollenberg and Hunten*, 1980; *Turco et al.*, 1983]. Haze is considered as an aerosol that impedes vision and may consists of droplets, and dust usually of size less than 1 $\mu$m. The clouds are generally thought of as a photochemical haze observed in the altitude range of 45–70 km. In situ probe measurements detected three cloud layers (upper, middle, and lower) based on distinctive cloud particle size distributions of $\sim$0.4, $\sim$2 and $\sim$7 $\mu$m [*Esposito et al.*, 1983; *Crisp et al.*, 1991; *Carlson et al.*, 1993; *Grinspoon et al.*, 1993]. The thick opaque cloud region between 48 and 56 km has been observed on Galileo and ground-based near-infrared images of Venus [*Crisp et al.*, 1989; *Bell et al.*, 1991; *Carlson et al.*, 1993; *Grinspoon et al.*, 1993]. Microphysical processes in the cloud layer are described in detail in various papers [e.g., *Toon et al.*, 1982; *James et al.*, 1997; *Imamura and Hashimoto*, 1998, 2001]. Two different mechanisms have been invoked to explain the formation of these clouds. Near the cloud top, photochemistry leads to the formation of cloud particles [*Krasnopolsky and Pollack*, 1994; *Mills and Allen*, 2007]; near the cloud base, condensation of sulfuric acid vapor on hydrated sulfuric acid particles may be responsible for the particle formation [*Young*, 1973; *Rossow*, 1978]. According to *Aplin* [2006], the sulfuric acid condensation onto ions also plays a role in the formation of cloud particles in 42–44 km region in the atmosphere. The cloud particles have a number density ranging from 100 to 1000 cm$^{-3}$ and the particle size distribution is bimodal [*Knollenberg and Hunten*, 1980; *Pollack et al.*, 1993; *Grinspoon et al.*, 1993; *Krasnopolsky*, 1989]. An upper haze layer is observed in the altitude range of 70 to 90 km, containing particles with an effective radius of 0.2–0.3 $\mu$m, composed of $H_2SO_4/H_2O$ aerosol with 75% sulfuric acid [*Kawabata et al.*, 1980]. A transport model between this haze layer and the atmospheric cloud is discussed by *Yamamoto and Takahashi* [2006]. The Venus Monitoring Camera (VMC) onboard Venus Express spacecraft investigated the global and small-scale properties of the upper cloud layer of Venus and found that the polar cloud pattern was highly variable on short time scales [*Markiewicz et al.*, 2007]. VMC also found that the polar haze expanded to the mid latitudes and the equatorial cloud showed wavy and streaky morphology [*Markiewicz et al.*, 2007]. The abundance and size distributions of the cloud and haze layers are shown in Figure 1.

[1] Department of Civil Engineering, Indian Institute of Technology, Kanpur, India.
[2] NASA Ames Research Center, Moffett Field, California, USA.
[3] SETI Research Institute, Mountain View, California, USA.


0148-0227/09/2008JE003258$09.00

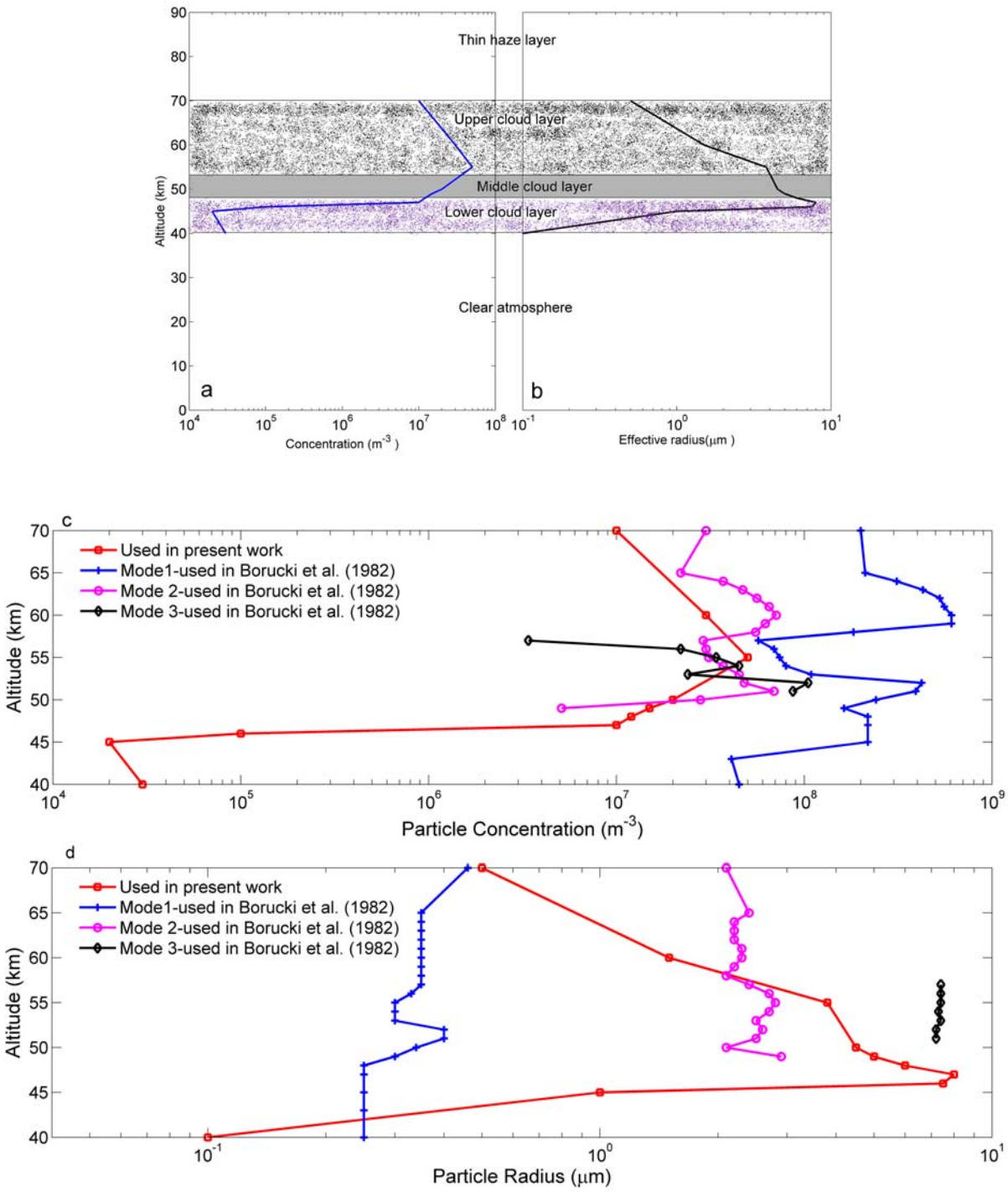


**Figure 1.** (a) Altitude profile of the size-integrated distribution and (b) effective particle radii [*James et al.*, 1997] along with the cloud layers. (c) Concentration and (d) radius of monodisperse cloud particles used in the present work are compared with those used by *Borucki et al.* [1982].

[3] The cloud particles are charged by the attachment of electrons to the particles and charge transfer from the ions. Attachment and charge transfer to particles is a loss mechanism for electrons and ions and causes a reduction in atmospheric electrical conductivity. Since the cloud cover is ubiquitous in the atmosphere of Venus, reduced conductivity is a global phenomenon. *Borucki et al.* [1982] have calculated the conductivity of the lower atmosphere of Venus, taking into account the then available data on the atmospheric environment and the cloud particles. Their study showed that the great abundance of cloud particles caused significant reductions of the conductivity within the clouds and has implications for lightning activity [*Borucki et al.*, 1982; *Russell*, 1991].

[4] Lightning is a large-scale electric discharge that occurs in the planetary atmospheres when the electric field reaches a critical value. In the Earth's atmosphere, lightning is produced by thunderclouds and most of the discharges occur within the clouds. Most discharges begin within the cloud where there are large concentrations of positive and negative space charge. Electrification intensifies as the convective activity increases, and becomes intense when there is rapid vertical growth of the cloud with the development of precipitation. Though the searches for the existence of lightning in Venus in the past have been both positive [*Krasnopolsky*, 1983; *Gurnett et al.*, 1991; *Hansell et al.*, 1995] and negative [*Sagdeev et al.*, 1986; *Borucki et al.*, 1991; *Gurnett et al.*, 2001], the recent observations by the Venus Express instruments detected strong, circularly polarized electromagnetic waves which have the expected properties of signals generated by lightning discharges [*Russell et al.*, 2007]. In the middle cloud layer, the temperature and pressure are almost Earth-like with a pressure close to 0.5 bar and a temperature of about 315 K. The clouds are thought to be composed of $H_2SO_4$ droplets, which are readily charged. Thus, lightning could occur if convection produces large potential differences within the clouds. *Russell et al.* [2007] also inferred that, in the Venusian atmosphere most discharges consist of intracloud strokes. The presence of lightning on Venus implies the existence of atmospheric regions in which charge separation mechanisms operate at a rate sufficient to overcome the dissipation of the separated charge by atmospheric conduction [*Borucki et al.*, 1982]. Atmospheric electrification at various bodies in the solar system has been reviewed by *Desch et al.* [2002] and *Aplin* [2006]. The review of *Yair et al.* [2008] suggested that there is a lack of modeling work to understand the charging of cloud particles and the production of lightning discharges.

[5] In this work, the influence of cloud particles on the conductivity profile of the lower atmosphere between 40 to 70 km is studied. The thin haze layer that exists above 70 km is too tenuous, and *Borucki et al.* [1982] calculated the reduction in atmospheric conductivity due to the presence of this haze to be not very significant (<15%).

[6] In order to study the conductivity of the atmosphere, it is necessary to understand the ion production rates, composition, concentration, mobility, attachment coefficients to particles, and concentration and size distribution of particles. The input data, the numerical method to calculate the steady state concentration of ions, electrons and cloud particles, and the results are discussed in the following sections. The present work uses more recent data on the atmospheric environment and particle characteristics than those used by *Borucki et al.* [1982]. A more efficient method is used in the present work to calculate the ion and electron charge transfer and attachment coefficients to particles. The present model considers a polydisperse distribution of particles, whereas *Borucki et al.* [1982] used one, two, or three monodisperse distributions varying with altitude. A Runge-Kutta method is used in the present study which is different than the numerical method used by *Borucki et al.* [1982]. All the differences and similarities of the input parameters and the results are compared with those of *Borucki et al.* [1982]. The implication of large charges on the cloud particles for lightning in the atmosphere of Venus is also discussed.

## 2. Ion Production

[7] *Chen and Nagy* [1978] have shown that the ionizing solar ultraviolet radiation does not penetrate much below ~120 km. Thus, below ~70 km (the region of interest of the present study) galactic cosmic rays (GCR) are the principal ionizing agent for the atmosphere. The incident radiation is mainly atomic nuclei, consisting of ~90% protons, ~10% He nuclei, and about l% heavier nuclei [*Upadhyay et al.*, 1994].

[8] The shape of the cosmic ray spectrum is such that a significant fraction of the total energy flux is carried by particles with kinetic energies above 1 GeV. *Borucki et al.* [1982] used the method developed by *O'Brien* [1970] to calculate the cosmic ray–induced ionization rates in the Venusian atmosphere. Ionization of the atmosphere by energetic particles produces primary ions $CO_2^+$, $CO^+$, and $O_2^+$ and electrons. Because the collision frequency with neutral species is large, the primary ions and electrons rapidly form secondary ions and ion clusters. The conductivity of the atmosphere is governed by the mobility of these long-lived secondary ions and ion clusters, rather than by the very mobile, but short-lived, primary ions and electrons. *Borucki et al.* [1982] estimated that ions such as $H_3O^+.SO_2$ (81 amu), $H_3O^+H_2O.CO_2$ (81 amu), $H_3O^+.(H_2O)_3$ (73 amu), and $H_3O^+.(H_2O)_4$ (91 amu) are the most abundant positive ion clusters and that these dominate the conductivity owing to positive ions. In the atmosphere of Venus, sulfur dioxide and oxygen are the major gaseous species to which free electrons may attach. $O_2^-$ readily transfers its charge to sulfur dioxide and the subsequent reactions of $SO_2^-$ are uncertain. The study of *Keesee et al.* [1980] suggested that $(SO_2)_2^-$ would prevail above about 25 km. A review of the cluster ions produced, their interaction with the particles and the atmospheric electrification is reported by *Aplin* [2006]. The ion production rates reported by *Borucki et al.* [1982], which has been considered the best estimate [*Aplin*, 2006], have been used in the present work for altitudes less than 70 km in the Venusian atmosphere; the mass of positive and negative ions clusters considered are 83 and 128 amu, respectively.

## 3. Venusian Clouds

[9] The clouds of Venus are generally thought of as a photochemical haze observed in the altitude range of 45–70 km. Droplets of $H_2SO_4$ + $H_2O$ were identified in the upper cloud layer from polarimetric observations [*Hansen and Hovenier*, 1974] who suggested an $H_2SO_4$ concentration of ~75 wt %. Spectroscopic observations by *Pollack et al.* [1978] showed that the concentration of $H_2SO_4$ is ~84 ± 2 wt % at the cloud tops, and the consistency of this concentration level with gaseous concentrations in the cloud top region has been emphasized recently by *Krasnopolsky* [2007]. The modeling study by *Krasnopolsky and Pollack* [1994] suggested that the $H_2SO_4$–$H_2O$ system in the Venus clouds has a constant $H_2SO_4$ concentration of 85 wt % for the sulfuric acid aerosols in the upper cloud layer, increasing to 98 wt % at the lower cloud boundary. Microphysical

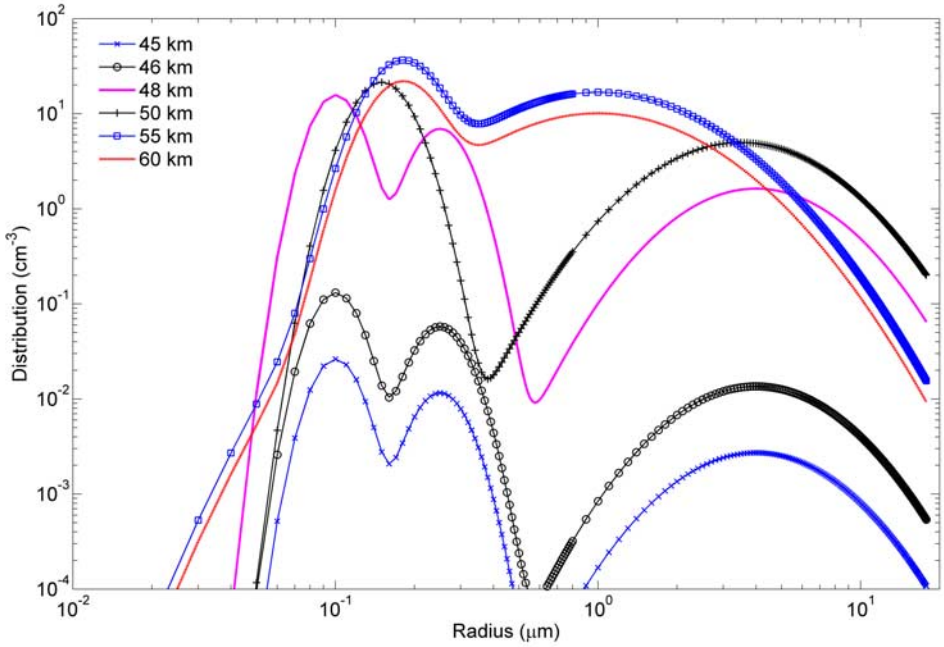


**Figure 2.** Polydisperse distribution of cloud particles at various altitudes.

processes in the cloud layer are described in detail in various papers [e.g., *Toon et al.*, 1982; *James et al.*, 1997; *Imamura and Hashimoto*, 1998, 2001].

[10] *James et al.* [1997] developed a numerical microphysical model of the condensational cloud of Venus, which treats vertical transport of sulfuric acid and water solution aerosols, their nucleation, growth, evaporation, coagulation, and sedimentation. The vertical profiles of sulfuric acid gas and water vapor, cloud microphysical properties and the acid concentration of the aerosol particles are predicted by the model of *James et al.* [1997] and are in agreement with Pioneer Venus observational data and Magellan radio occultation data. They found that the lower Venus cloud is formed as a consequence of a large upward flux of sulfuric acid vapor from the evaporation region below the cloud base and that the heterogeneous nucleation of sulfuric acid and water vapors is a plausible mechanism for the formation of the lower cloud in the atmosphere of Venus. The size distribution of cloud particles is approximately bimodal in the middle cloud and trimodal in the lower cloud. The smallest mode is formed by cloud condensation nuclei diffused from below the cloud. The largest mode is formed by cloud droplets nucleated near the top of the cloud. The droplets continue to grow while sedimenting; thus, the mean size of this mode increases toward the bottom of the cloud. The middle mode, present in the lower cloud, is a result of heterogeneous nucleation on soluble cores. The aerosols that contain enough soluble material to reduce the vapor pressure significantly are activated to become cloud droplets and form this mode. Those containing less soluble material remain behind as aerosols of the smallest mode [*James et al.*, 1997].

[11] In the present work, the lower cloud region is considered to be the altitude region from 40 to 48 km, the middle cloud as the altitude region 49 to 52 km, and the upper cloud as the altitude region from 53 to 70 km. A schematic of the cloud layers is presented in Figures 1a and 1b. The lower cloud layer is considered to have a trimodal distribution of particles while the middle and upper layers are considered bimodal. *James et al.* [1997] reported the lognormal distribution of cloud particles at various altitudes corresponding to the lower, middle, and upper cloud layers. These distributions are used in the present work for the altitudes considered in the model corresponding to the lower, middle, and upper cloud layers. The effective radii of particles (0.02 to 10 $\mu$m) are divided into 10 bins in a geometric progression. The abundance and size distribution of particles which are observed by the Pioneer Venus

**Table 1.** Properties of Polydisperse Distribution of Cloud Particles[a]

| | Mode 1 | | Mode 2 | | Mode 3 | |
|---|---|---|---|---|---|---|
| | $r_m$ ($\mu$m) | $\sigma$ | $r_m$ ($\mu$m) | $\sigma$ | $r_m$ ($\mu$m) | $\sigma$ |
| Lower cloud (40–48 km) | 0.10 | 1.20 | 0.25 | 1.23 | 4.00 | 1.80 |
| Middle cloud (49–52 km) | 0.15 | 1.25 | 3.50 | 1.90 | - | - |
| Upper cloud (53–70 km) | 0.18 | 1.29 | 1.00 | 2.16 | - | - |

[a]Mode 1, mode 2, and mode 3 are lognormal distributions, $N(r) = (N/(\sqrt{2\pi} r \ln \sigma)) \exp[-(\ln r - \ln r_m)^2/(2\ln^2 \sigma)]$. The mean radius is $r_m$, and the standard deviation is $\sigma$.

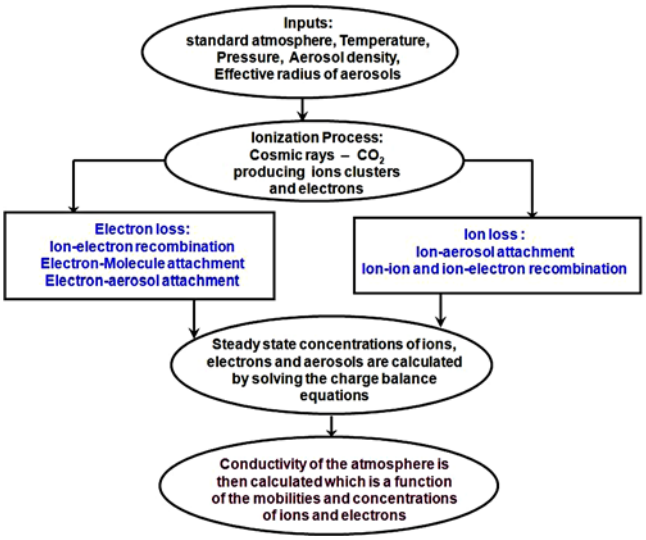


**Figure 3.** Flow diagram of the charging calculation of aerosols in the atmosphere of Venus.

instruments [*Knollenberg and Hunten*, 1980] are modeled by *James et al.* [1997] and are used in the present study (see Figures 1a and 1b, respectively). The particle concentration and effective radii used by *Borucki et al.* [1982] are compared with those used in the present work and are presented in Figures 1c and 1d, respectively. The polydisperse distribution generated is presented in Figure 2, and the parameters are presented in Table 1. This distribution is superior to those three monodisperse distributions of particles used by *Borucki et al.* [1982], where the radii remain almost a constant for each distribution.

## 4. Description of the Model and Method of Calculation

[12] The flow diagram of the model for the charging of particles by the attachment of ions and electrons is presented in Figure 3. The basic inputs to the model are the standard atmosphere (temperature and pressure), aerosol abundance, and effective radii of aerosols. The aerosol abundance and the effective radii were discussed in section 3. The production of ions and electrons by the interaction of GCR was discussed in section 2. The neutral number density and temperature profiles are taken from *Krasnopolsky* [2007] and *Bertaux et al.* [2007] and are provided in Figures 4 and 5. The neutral number density and temperature are similar to those used by *Borucki et al.* [1982] as shown in Figures 4 and 5. The ion mobility and the ion mean free path agree very well with those used by *Borucki et al.* [1982]. The ion-ion recombination coefficient is calculated using the method of *Hua and Holzworth* [1996] and is within 20% of that used in the work of *Borucki et al.* [1982] for regions where clouds are present (40 to 70 km). *Tinsley and Zhou* [2006] used a different expression to calculate the ion-ion recombination coefficient and found to be in the same order of magnitude as used in the present study and using their expression does not alter the atmospheric conductivity significantly (<10%). The electron-ion recombination coefficient and the electron

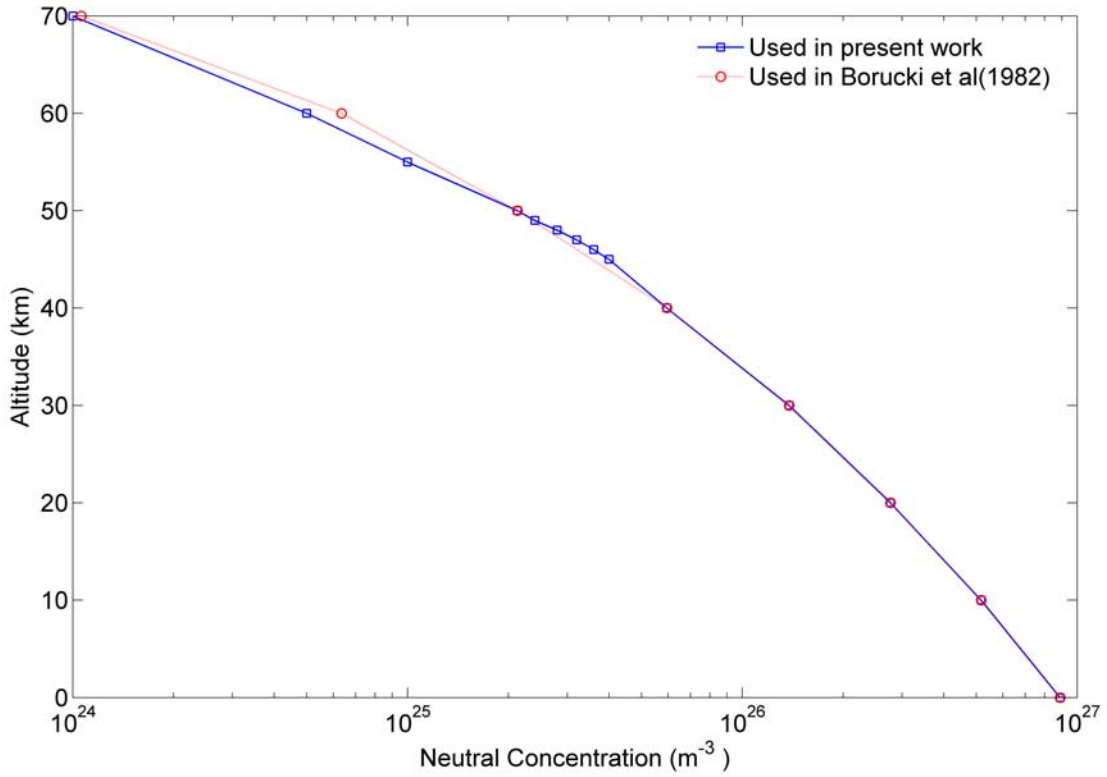


**Figure 4.** Neutral concentration of the atmosphere of Venus used in the present study compared with that used by *Borucki et al.* [1982].

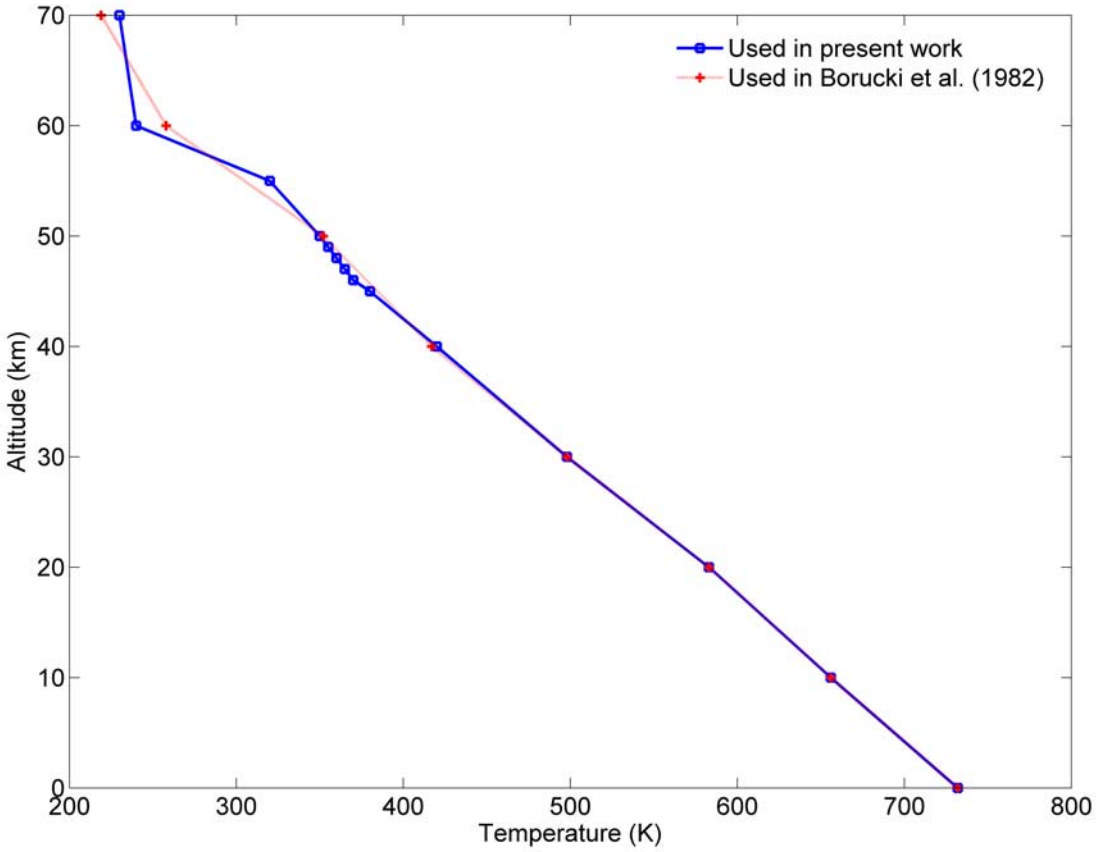


**Figure 5.** Temperature profile of the atmosphere of Venus used in the present study compared with those used by *Borucki et al.* [1982].

detachment coefficients are similar to those calculated by *Borucki et al.* [1982]. The ion charge transfer and electron attachment coefficients are calculated using the method developed by *Hoppel and Frick* [1986]. This calculation is discussed by *Michael et al.* [2007, 2008], *Tripathi and Michael* [2008], and *Tripathi et al.* [2008]. The typical values of these coefficients of positive ions, negative ions and electrons at 55 km in the atmosphere of Venus are provided in Figures 6a–6c, respectively and those at 49 km are presented in Table 2. The attachment and charge transfer

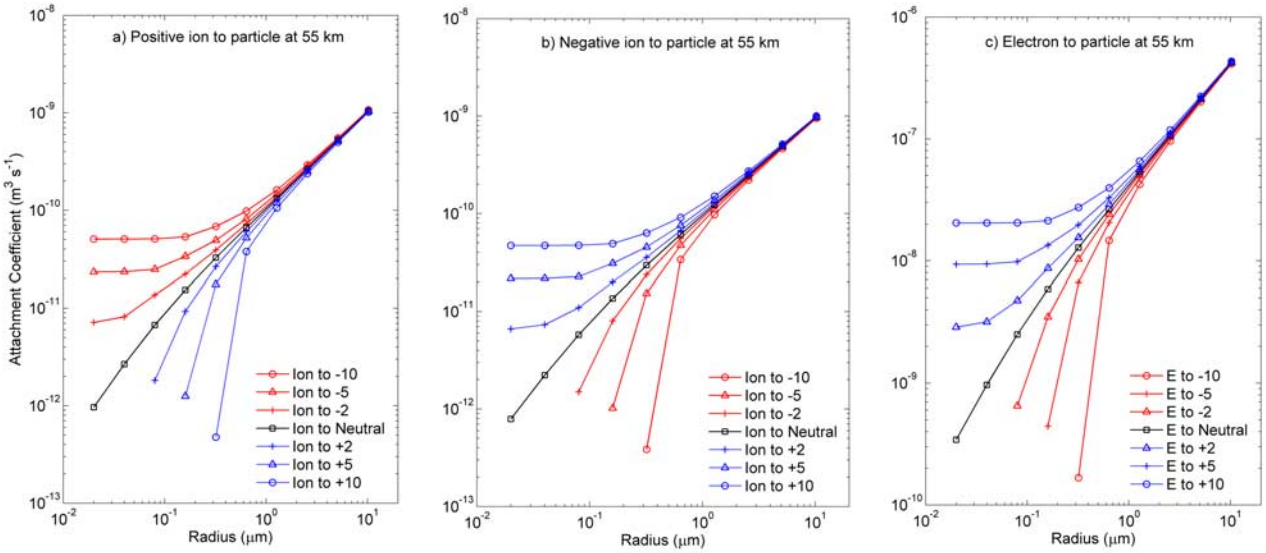


**Figure 6.** (a) Positive ion to particle, (b) negative ion to particle, and (c) electron to particle attachment coefficient at 55 km. Ion to −10 and E to −10 in the legend represent the attachment coefficient of the ions and electrons, respectively, to the particle with charge −10e.

**Table 2.** Attachment Coefficient $\beta$ of Positive Ions, Negative Ions, and Electrons to Cloud Particles at 49 km

| | Radius ($\mu$m) | | | | | | |
|---|---|---|---|---|---|---|---|
| $\beta^a$ ($m^3$ $s^{-1}$) | 0.02 | 0.08 | 0.16 | 0.64 | 1.28 | 5.12 | 10.24 |
| | | | | *Positive Ions* | | | |
| −10 | 3.23E-11[b] | 3.25E-11 | 3.46E-11 | 6.60E-11 | 1.11E-10 | 3.81E-10 | 7.40E-10 |
| −5 | 1.55E-11 | 1.67E-11 | 2.25E-11 | 5.61E-11 | 1.02E-10 | 3.73E-10 | 7.32E-10 |
| −2 | 5.35E-12 | 9.79E-12 | 1.57E-11 | 5.05E-11 | 9.63E-11 | 3.68E-10 | 7.27E-10 |
| 0 | 8.95E-13 | 5.37E-12 | 1.15E-11 | 4.68E-11 | 9.28E-11 | 3.64E-10 | 7.23E-10 |
| 2 | 0.00E+00 | 1.86E-12 | 7.70E-12 | 4.34E-11 | 8.95E-11 | 3.61E-10 | 7.20E-10 |
| 5 | 0.00E+00 | 0.00E+00 | 2.11E-12 | 3.83E-11 | 8.45E-11 | 3.56E-10 | 7.15E-10 |
| 10 | 0.00E+00 | 0.00E+00 | 0.00E+00 | 2.99E-11 | 7.65E-11 | 3.48E-10 | 7.07E-10 |
| | | | | *Negative Ions* | | | |
| −10 | 0.00E+00 | 0.00E+00 | 0.00E+00 | 2.72E-11 | 7.09E-11 | 3.26E-10 | 6.62E-10 |
| −5 | 0.00E+00 | 0.00E+00 | 1.75E-12 | 3.52E-11 | 7.85E-11 | 3.33E-10 | 6.70E-10 |
| −2 | 0.00E+00 | 1.56E-12 | 6.78E-12 | 4.00E-11 | 8.32E-11 | 3.38E-10 | 6.74E-10 |
| 0 | 7.42E-13 | 4.70E-12 | 1.03E-11 | 4.33E-11 | 8.64E-11 | 3.41E-10 | 6.77E-10 |
| 2 | 5.01E-12 | 8.14E-12 | 1.43E-11 | 4.68E-11 | 8.97E-11 | 3.44E-10 | 6.80E-10 |
| 5 | 1.45E-11 | 1.54E-11 | 2.08E-11 | 5.21E-11 | 9.46E-11 | 3.49E-10 | 6.85E-10 |
| 10 | 3.02E-11 | 3.03E-11 | 3.20E-11 | 6.14E-11 | 1.03E-10 | 3.57E-10 | 6.93E-10 |
| | | | | *Electrons* | | | |
| −10 | 0.00E+00 | 0.00E+00 | 0.00E+00 | 1.18E-08 | 3.08E-08 | 1.41E-07 | 2.87E-07 |
| −5 | 0.00E+00 | 0.00E+00 | 7.61E-10 | 1.53E-08 | 3.41E-08 | 1.45E-07 | 2.91E-07 |
| −2 | 0.00E+00 | 6.77E-10 | 2.94E-09 | 1.74E-08 | 3.61E-08 | 1.47E-07 | 2.93E-07 |
| 0 | 3.22E-10 | 2.04E-09 | 4.49E-09 | 1.88E-08 | 3.75E-08 | 1.48E-07 | 2.94E-07 |
| 2 | 2.18E-09 | 3.53E-09 | 6.19E-09 | 2.03E-08 | 3.89E-08 | 1.49E-07 | 2.95E-07 |
| 5 | 6.28E-09 | 6.68E-09 | 9.03E-09 | 2.26E-08 | 4.11E-08 | 1.51E-07 | 2.97E-07 |
| 10 | 1.31E-08 | 1.32E-08 | 1.39E-08 | 2.67E-08 | 4.48E-08 | 1.55E-07 | 3.01E-07 |

[a]The $\beta$ values of −10, −5, etc., represent the attachment coefficient of positive ions, negative ions, and electrons, respectively, to the particles of charge −10e, −5e.
[b]Read 3.23E-11 as $3.23 \times 10^{-11}$.

coefficients are in very good agreement (within 10%) with those of *Borucki et al.* [1982] in the diffusive regime (below 60 km). *Hoppel* [1985] and *Hoppel and Frick* [1986] calculated the ion-aerosol attachment coefficients in the terrestrial atmosphere and are found to be within 20% of those calculated for particles of similar size in the atmosphere of Venus.

[13] The concentrations of ions, electrons and aerosols can be found from the charge balance equations. These constitute a set of $(2s + 1) \times k + 3$ simultaneous differential equations, where $s$ is the maximum number of elementary charges allowed on a particle and k is the radius index of polydisperse particles [*Yair and Levin*, 1989]. The ion and electron charge balance equations can thus be written as

$$\frac{dn^+}{dt} = q - \alpha n^+ n^- - \alpha_e n^+ n^e - n^+ \sum_i \sum_k \beta_{1k}^{(i)} N_k^i \qquad (1)$$

$$\frac{dn^-}{dt} = \beta_j n_j n^e - \alpha n^+ n^- - n^- \sum_i \sum_k \beta_{2k}^{(i)} N_k^i - F n^- \qquad (2)$$

$$\frac{dn^e}{dt} = q - \alpha_e n^+ n^e - \beta_j n_j n^e - n^e \sum_i \sum_k \beta_{ek}^{(i)} N_k^i + F n^- \qquad (3)$$

Here, $q$ is the ion production rate (which is the same for the positive ions and electrons), $\alpha$ is the ion-ion recombination coefficient, $\alpha_e$ is the electron-ion recombination coefficient, $\beta_{mk}^i$ is the charge transfer coefficient for ions of polarity $m$ (1 for positive and 2 for negative) to particles with charge $i$ and the radius index $k$, $\beta_{ek}^i$ is the electron attachment coefficient to particles with charge $i$ and radius index $k$, $\beta_j$ is the electron attachment coefficient to neutral species $n_j$, and $N_k^i$ is the density of particles of charge $i$ and radius index $k$. $\beta_j$ is estimated as $1 \times 10^{-21}$ $m^3$ $s^{-1}$ on the basis of the work of *Christophorou* [1980]. $F$ represents the collisional detachment of electrons from negative ions and is evaluated using the equation from *Arnold* [1964] and found to be negligible in the 40 to 70 altitude region.

$$F \approx p\pi^{1/2} \frac{L_m}{L_I} \frac{P}{KT} \sigma^2 \left(\frac{8KT}{\pi m}\right)^{1/2} \left(\frac{E_a}{KT} + 1\right) \exp\left(-\frac{E_a}{KT}\right) \qquad (4)$$

Here $p$ is the probability of an energetic collision removing an electron (~0.02), $L_M/L_I$ is the ratio of the mean free path of neutral molecules to that of ions, $P$ is the pressure, $\sigma$ is the collision cross section (~$10^{-8}$ $cm^2$), $E_a$ is the electron affinity of the negative ions (~2 eV), $m$ is the mass of the negative ions, $k$ is the Boltzmann constant, and $T$ is the temperature.

[14] *Parthasarathy* [1976] derived a steady state recurrence relation to compute the buildup of electric charge on aerosol particles due to collision with positive and negative ions and electrons. *Jensen and Thomas* [1991] reported a method for computing electron attachment and ion charge transfer coefficients. *Whitten et al.* [2007] modified the recurrence expression given by *Parthasarathy* [1976] to estimate the charge distribution on aerosols and developed the method to evaluate the time dependence of the charge accumulation by aerosols. The time dependant charge balance equations for the aerosols are

$$\frac{dN_k^i}{dt} = \beta_{1k}^{(i-1)} n^+ N_k^{(i-1)} + \beta_{2k}^{(i+1)} n^- N_k^{(i+1)} + \beta_{ek}^{i+1} n^e N_k^{(i+1)} - \beta_{1k}^{(i)} n^+ N_k^i - \beta_{2k}^{(i)} n^- N_k^i - \beta_{ek}^i n^e N_k^i \qquad (5)$$

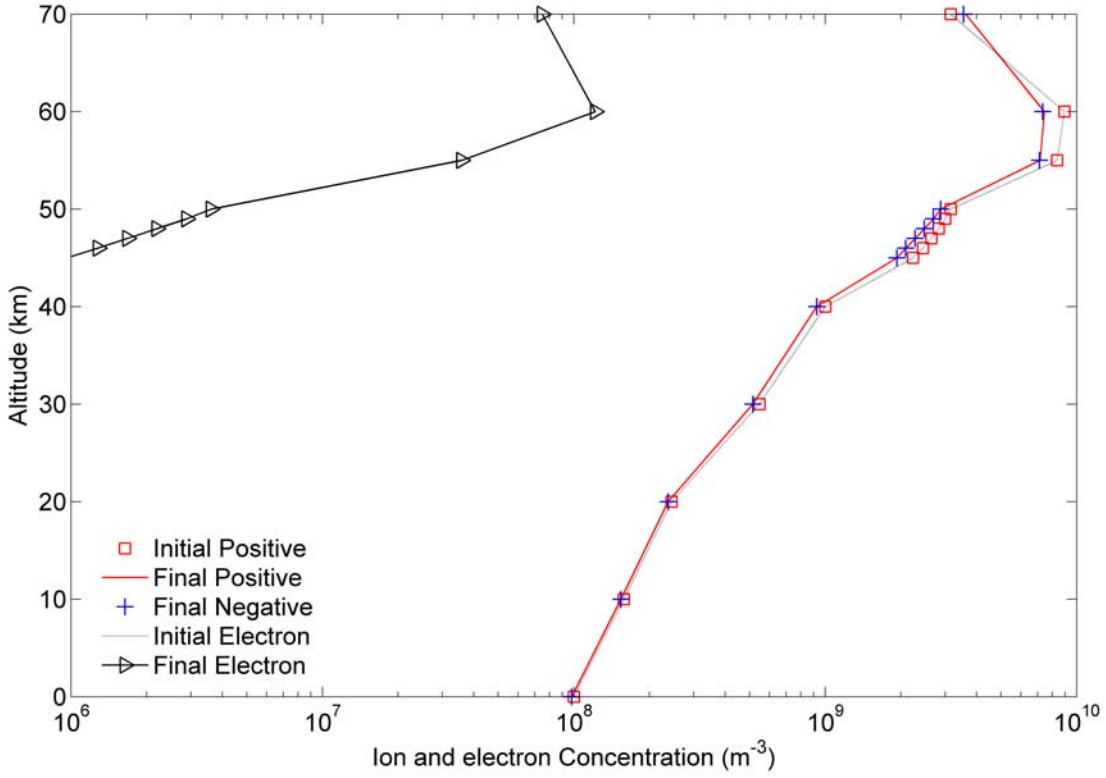


**Figure 7.** Variation in the ion and electron concentration in the absence of cloud particles.

The differential equations are solved using the fourth-order Runge-Kutta method. This method numerically integrates ordinary differential equations by using a trial step at the midpoint of an interval to cancel out lower-order error terms. This approach is used to solve the set of equations at every altitude using the charge conservation as a constraint on the calculations:

$$zp + n^+ - n^- - n^e = 0 \tag{6}$$

Here $n^+$, $n^-$ and $n^e$ are the positive, negative ions and electrons densities, respectively and $zp$ is the total charge on the aerosols which is expressed as

$$zp = \sum_p pN_p \tag{7}$$

where $N_p$ is the density of aerosols with charge state $p$. The altitudes between 40 and 70 km are divided into 14 bins with 1 km bin where the cloud particle concentration and radii are changing rapidly. A similar numerical method was used to estimate the aerosol charging in the nighttime and daytime atmosphere of Mars [*Michael et al.*, 2007, 2008], during Martian dust storms [*Michael and Tripathi*, 2008], in the atmosphere of Titan [*Borucki et al.*, 2006; *Whitten et al.*, 2007], and in the atmosphere of Jupiter [*Whitten et al.*, 2008].

[15] After steady state is achieved, the conductivity of the atmosphere is calculated as

$$\sigma = e(n^+K_+ + n^-K_- + n^eK_e) \tag{8}$$

where, e is the electronic charge, $n^+$, $n^-$ and $n^e$ are the number densities of ions and electrons and the $K_+$, $K_-$, and $K_e$ are the corresponding mobilities.

[16] Initially the concentrations of positive ions and electrons are considered equal and estimated as $(q/\alpha_e)^{0.5}$. Negative ions are formed by the attachment of electrons to the neutrals. Ions and electrons are lost by the ion-ion recombination, ion-electron recombination, and charge transfer to cloud particles. Negative ions are also lost by detachment of electrons from ions also. As shown by *Borucki et al.* [1982] electron detachment is important only at the lower altitudes. To understand the effect of these processes alone, the calculations were carried out in the absence of cloud particles keeping equal concentration of positive ions and electrons and no negative ions initially. *i.e.* the summation terms in equations (1), (2), and (3) are assumed to be zero. The variation in the ion and electron concentrations is depicted in Figure 7.

[17] It is clear that most of the electrons are lost in the lower atmosphere (below 40 km) to produce negative ions by the attachment of electrons to neutrals. The electron concentration peaks at ~60 km. For altitudes greater than 60 km, the electron abundance is within 2 orders of magnitude than that of ions and therefore they significantly affect the conductivity of the atmosphere because their mobility is 100 times higher than that of the ions. The following subsections describe the consequence of charging of particles on conductivity when the additions of monodisperse and polydisperse distributions are considered. The

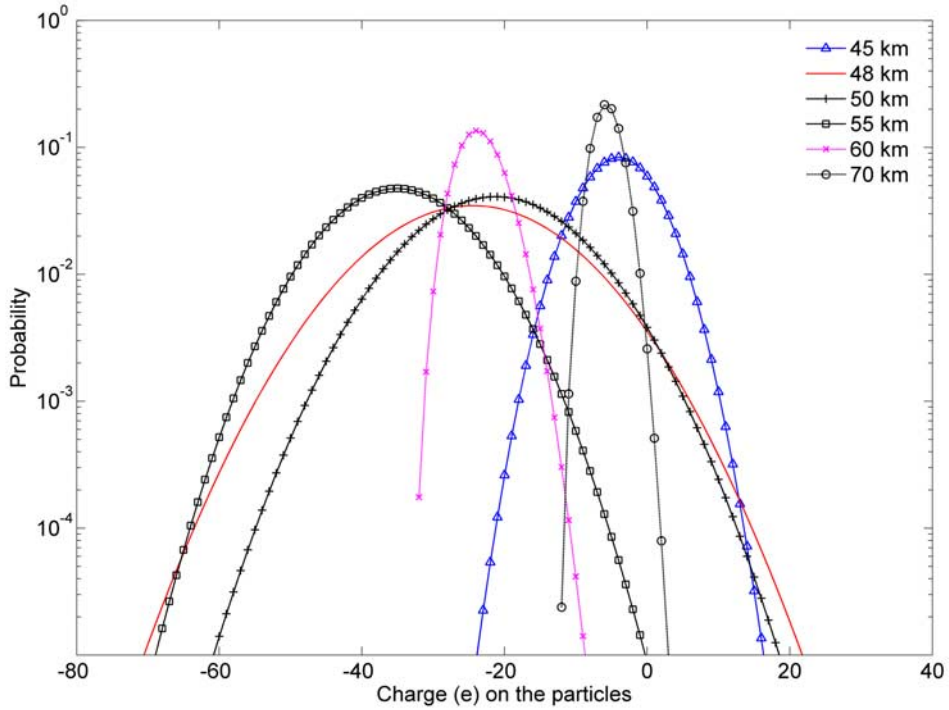


**Figure 8a.** Probability of charging of cloud particles at various altitudes using monodisperse distribution of particles.

implications of these charging to the lightning in the atmosphere are also discussed.

## 5. Results and Discussion

### 5.1. Monodisperse Distribution

[18] The calculations were carried out using the particle concentration and effective radius as shown in Figures 1a and 1b. For the monodisperse distributions considered, the summation over $k$ is removed in equations (1), (2), (3), and (5) since the radius of the particles is considered constant for a given altitude. Figure 8a presents charge distribution in terms of probability at a few altitudes in the atmosphere. The charge distribution is calculated as the ratio of the concentration of particles in a charge bin to the total concentration of particles at a given altitude. At 45 km, the charge distribution over the particles is almost symmetric as the concentrations of positive and negative ions are almost equal and the electron concentration is about 3 orders of magnitude smaller than the ion concentrations. As the altitude increases (up to 55 km) the electron concentration increases and there is an enhancement in the fraction of negatively charged particles. Though the electron concentration is higher at 60 km, the particle size decreases and therefore the attachment coefficient decreases. Consequently the particle charging decreases as depicted in Figure 8a. A similar situation obtains at 70 km. Figure 8b presents the mean charge per particle at each altitude.

[19] Figure 9 presents the charge distribution on particles for the 40 to 70 km altitude range. The concentration is presented on a logarithmic scale in the color map. It is clear that the maximum charge accumulation to the particles occurs at altitudes between 45 and 50 km, where large particles exist. The concentration of negatively charged particles peaks at 40 charges on the particles at 55 km owing to the effect of highly mobile electrons. Similarly, the higher concentration of negatively charged particles at 60 km is also attributed to the presence of electrons. The charge distribution is almost symmetric at altitudes less than 45 km and greater than 65 km as there are almost equally mobile positive and negative ions present in equal number and the concentration of electrons are ~3 to 4 orders of magnitude less than that of the ions.

[20] Figure 10 presents the variation in the concentrations of ions and electrons due to the attachment to cloud particles. The concentration of negative ions is assumed zero initially and therefore is not shown. Negative ions are produced by the electron attachment to neutrals and are lost by charge transfer to particles. To understand the effect of particle charge transfer on negative ions, the concentration of negative ions in Figure 10 is compared with that in Figure 7. There is a reduction in the ion concentration at altitudes between 45 and 70 km, which is qualitatively similar to the results of *Borucki et al.* [1982]. The maximum reduction in the ion concentration occurs at 50 km, a trend similar to that of *Borucki et al.* [1982]. The present study shows that the negative and positive ion concentrations decreased by factors 5 and 3, respectively at 50 km. The ion concentrations estimated by *Borucki et al.* [1982] denote that a reduction of about an order of magnitude occurs at 50 km. This difference can be attributed to the utilization of updated particle profile. The total surface area of particles is about an order of magnitude less than that used by *Borucki et al.* [1982] which reduces the rate of attachment of ions to particles.

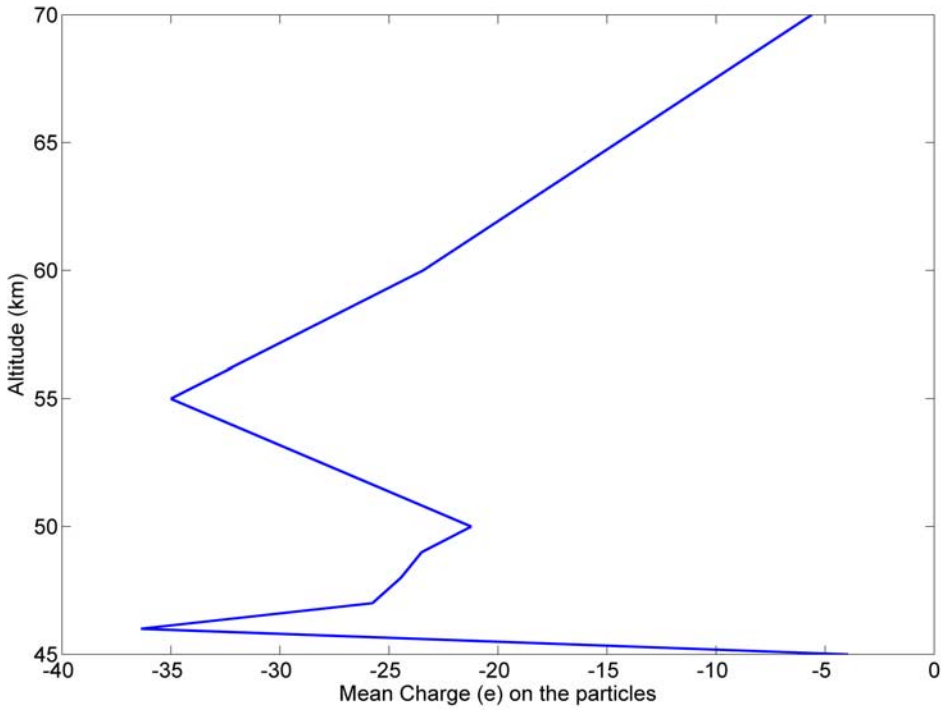


**Figure 8b.** Mean charge per cloud particle at various altitudes using monodisperse distribution of particles.

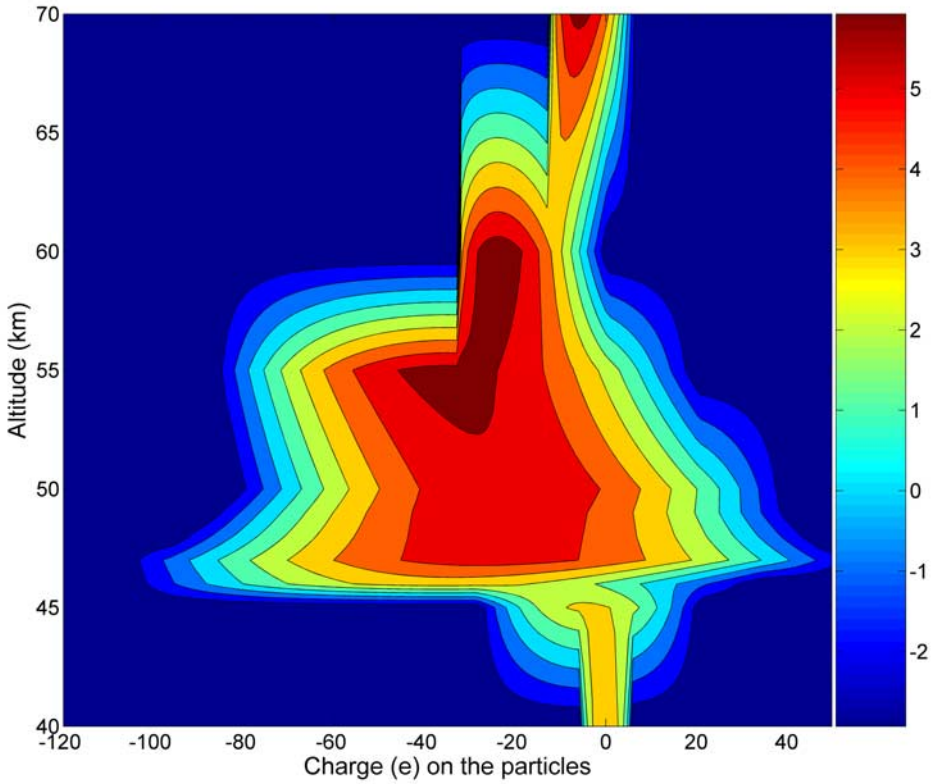


**Figure 9.** Charge distribution on cloud particles for monodisperse distribution. The *x* axis represents the electronic charge on the particles. Color scale is the logarithm of the concentration of particles in $m^{-3}$.

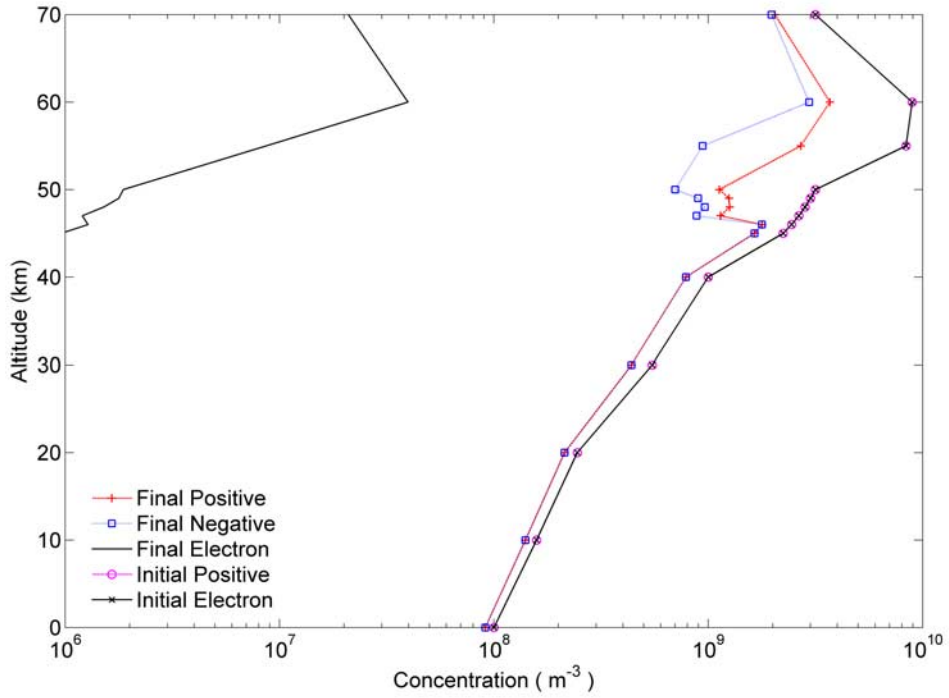


**Figure 10.** Initial and final concentrations of ions and electrons with the monodisperse distribution of cloud particles.

### 5.2. Polydisperse Distribution

[21] In the polydisperse distribution of particles, the radii of particles spread over the range of 0.02 $\mu$m to 10 $\mu$m as given in Figure 2. The steady state charge distribution at 46 km (lower cloud) is presented in Figure 11. It is seen that in the lower size region, the probability of particles acquiring charges more than 2 charges is very small while the probability of neutral particles is greatly increased. Larger particles have a higher probability of acquiring more charges. Ion-particle attachment coefficients play a role here

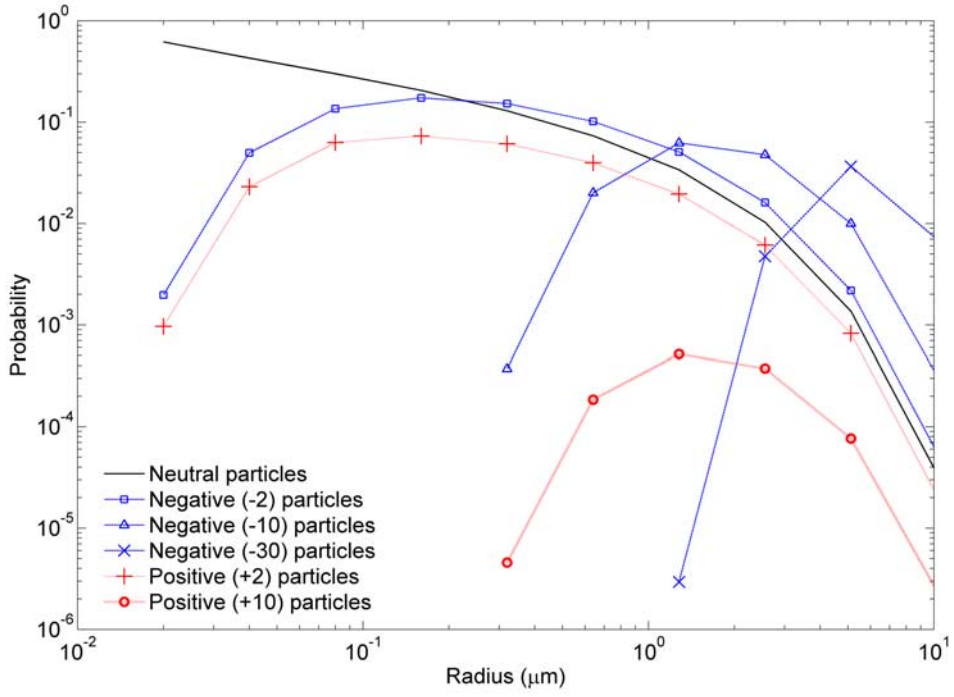


**Figure 11.** Probability of cloud particle charging at 46 km for polydisperse distribution. Negative (−2) particles in the legend means the probability to accumulate two negative charges on a particle.

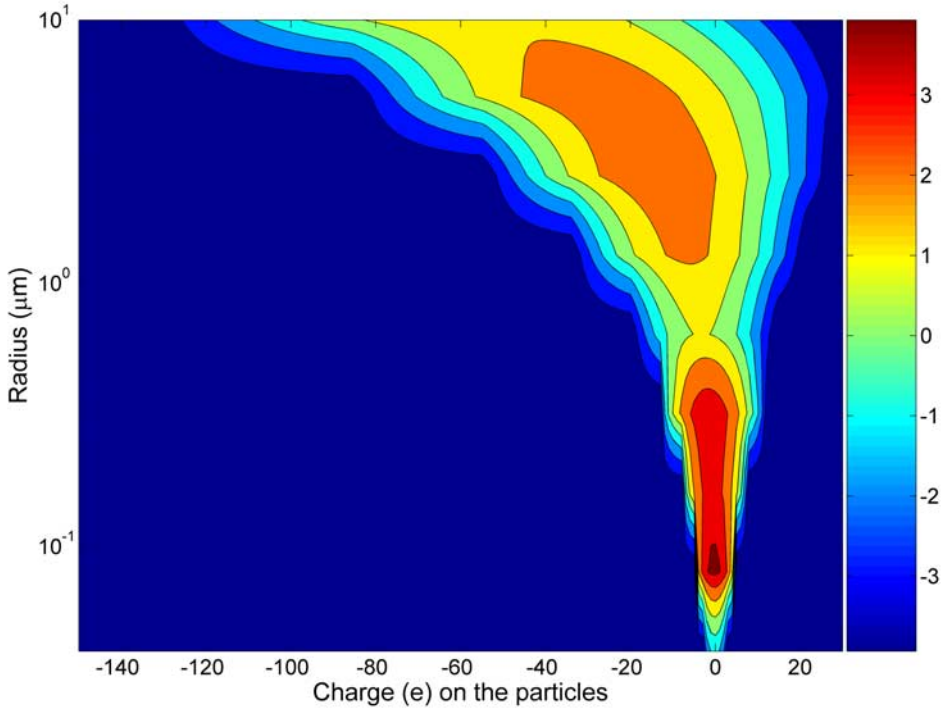


**Figure 12.** Charge distribution on cloud particles at 46 km with polydisperse distribution. The $x$ axis represents the electronic charge on the particles. Color scale is the logarithm of the particle concentration in $m^{-3}$.

as for smaller particles the attachment coefficients are much smaller than that of the larger particles as depicted in Figures 6a–6c. The ratio of the charge on a particle to the radius of the particle is calculated and found that the ratio is almost independent of the radius of the particle. It implies that larger particles accumulate greater number of charges as their attachment coefficient is higher. It can also be noted that more negatively charged particles are created than positively charged ones at all radius bins. The higher concentration of negatively charged particles is attributed to the presence of highly mobile electrons, though in lower abundance.

[22] Figure 12 presents the contour of the charge distribution of particles at 46 km. The color map is the logarithm of the concentration of particles. The charge distribution skews toward the negative side for bigger particles owing to the presence of highly mobile electrons and also owing to the higher attachment coefficients.

[23] Figures 13 and 14 are similar to Figures 11 and 12 for 49 km (middle cloud). It is evident from Figure 13 that the probability of the bigger particles accumulating large number of charges is higher than that of smaller particles owing to the higher attachment rates. The contour presented in Figure 14 shows that the maximum concentration inclines toward the negative side for larger particles owing to the presence of highly mobile electrons. *Chauzy and Despieu* [1980] measured the charge accumulated by the rain drops in the terrestrial atmosphere and found that larger drops carried more negative charges.

[24] Similarly, Figures 15 and 16 present the probability of charging and the charge distribution at 55 km (upper cloud). It is clear from Figure 15 that even for particles of size 0.1 $\mu$m, the probability of particles being negatively charged is greater than that of remaining neutral, contrary to that in the middle and lower cloud. This is due to the presence of the highly mobile electron at a higher concentration at this altitude. All particles have a higher probability for being negatively charged than positively charged. The contours in the Figure 16 show the very large negative charges accumulated by the bigger particles.

[25] Figure 17 presents the initial and final concentrations of ions and electrons. The altitude profile is qualitatively similar to the case of monodisperse distribution and that of *Borucki et al.* [1982]. The maximum reduction in the ion concentration occurs at 50 km in agreement with that of the monodisperse case and that of *Borucki et al.* [1982].

[26] The magnitude of reduction for the polydisperse case is smaller (by a factor of 2 to 3) than that of the case of monodisperse distribution because the particles are distributed over a wide range of radii and the resulting attachment rate is much smaller than the case that assumes all the particles are of bigger size. The effective attachment coefficient of the polydisperse particles was calculated and compared with that of the monodisperse particles. It was found that the attachment rate for the monodisperse particles was higher up to a factor of 6 than that of the polydisperse case.

[27] Figure 18 presents the conductivity of the atmosphere calculated using equation (8). To understand the significance of cloud particles, the calculations were carried out in the presence and absence of particles. The conductivity of the atmosphere with the monodisperse distribution of particles shows a similar trend to *Borucki et al.* [1982], where maximum reduction in conductivity occurs at

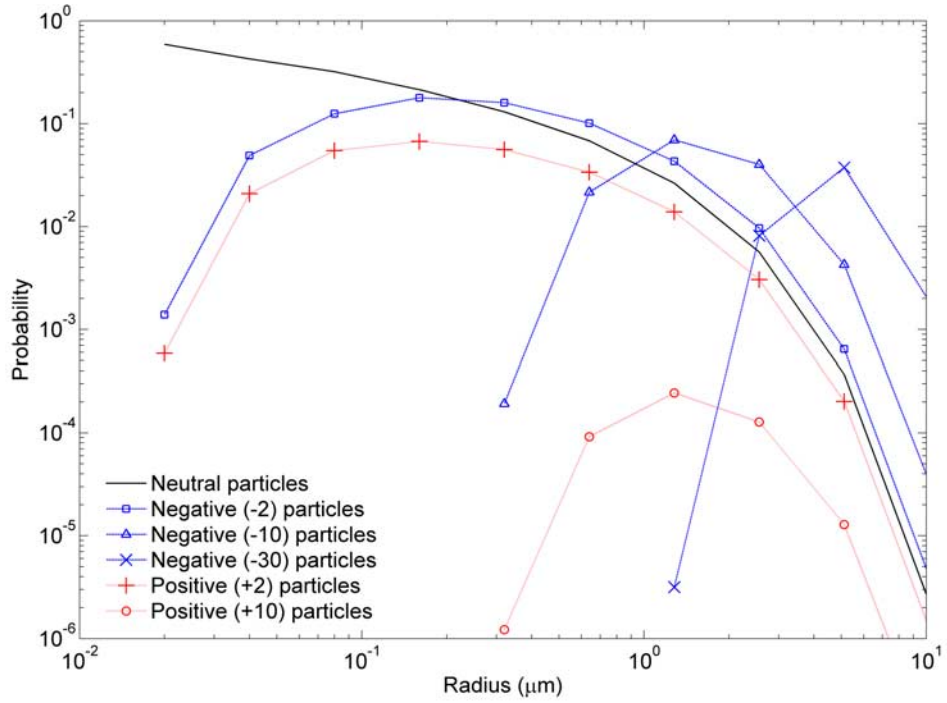


**Figure 13.** Probability of cloud particle charging at 49 km for polydisperse distribution. Negative (−2) particles in the legend means the probability to accumulate two negative charges on a particle.

∼50 km, with decreasing influence of cloud particles at altitudes greater than 50 km. The magnitude of reduction in the conductivity at 50 km (factor of ∼3) is smaller in the present work than reported by *Borucki et al.* [1982] (∼ an order of magnitude). This is probably because the total surface area of particles is about an order of magnitude less than that used by *Borucki et al.* [1982] which reduces the rate of attachment of ions to particles.

[28] Another interesting aspect to note is that, with polydisperse distribution of particles, the drop in conduc-

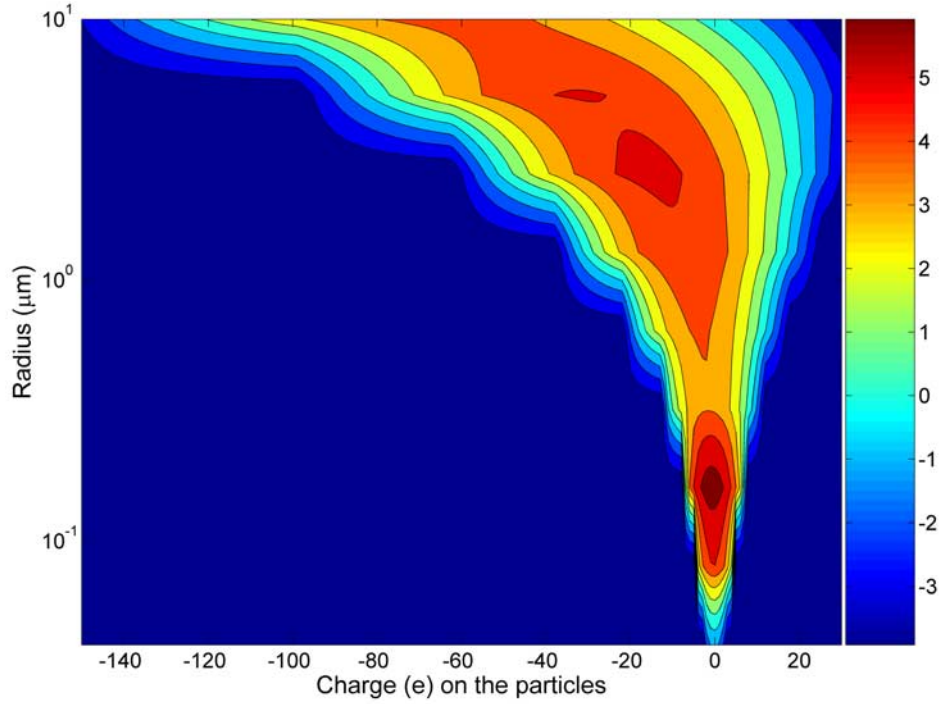


**Figure 14.** Charge distribution on cloud particles at 49 km with polydisperse distribution. The *x* axis represents the electronic charge on the particles. Color scale is the logarithm of the particle concentration.

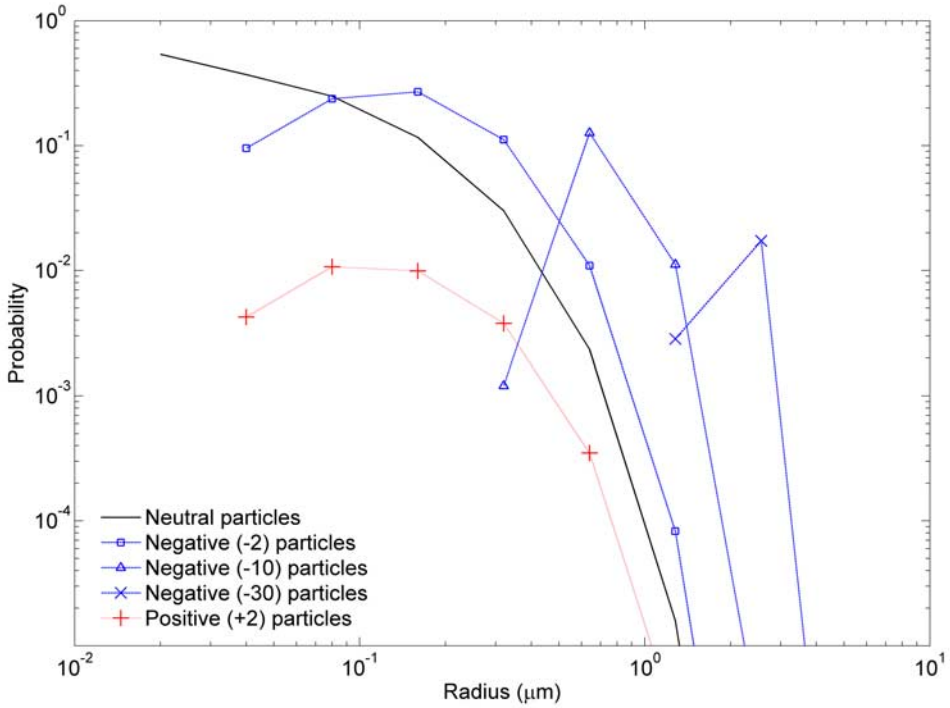


**Figure 15.** Probability of cloud particle charging at 55 km for polydisperse distribution.

tivity is lesser than the monodisperse case. At 50 km, where the effect is maximum, the conductivity was reduced by only about a factor of 2. The polydisperse distribution of cloud particles, which is a more realistic scenario, considers particles distributed over a size range of 0.02 $\mu$m to 10 $\mu$m, whereas in the monodisperse case all the particles are of the size $\sim$8 $\mu$m. As the attachment coefficients are larger for bigger particles, the attachment rate is much larger, while

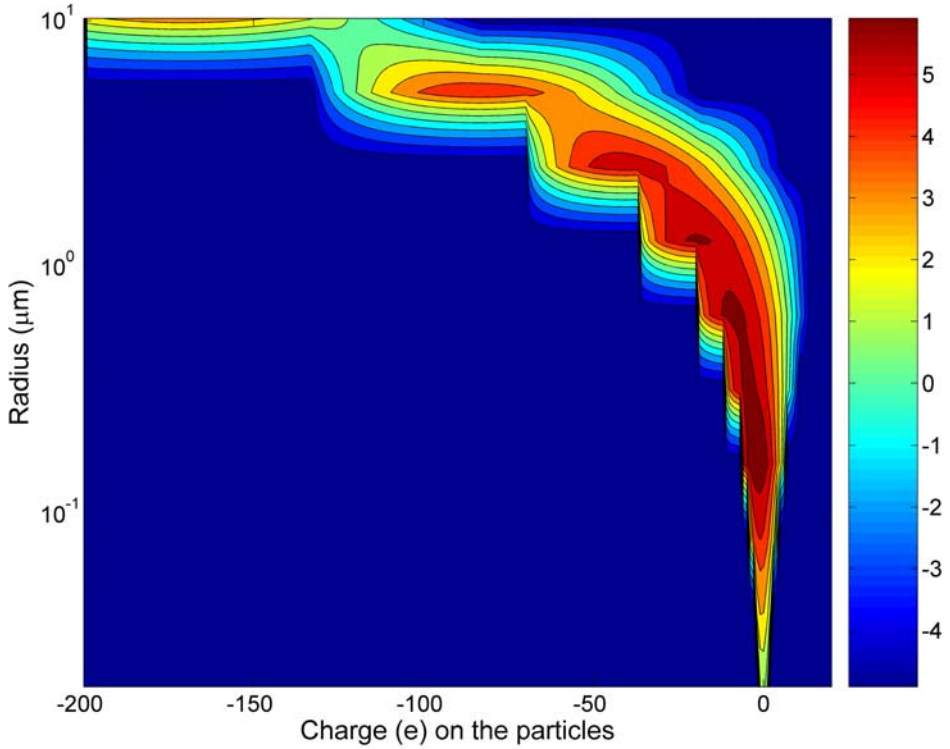


**Figure 16.** Charge distribution on cloud particles at 55 km with polydisperse distribution. The $x$ axis represents the electronic charge on the particles. Color scale is the logarithm of the particle concentration in $m^{-3}$.

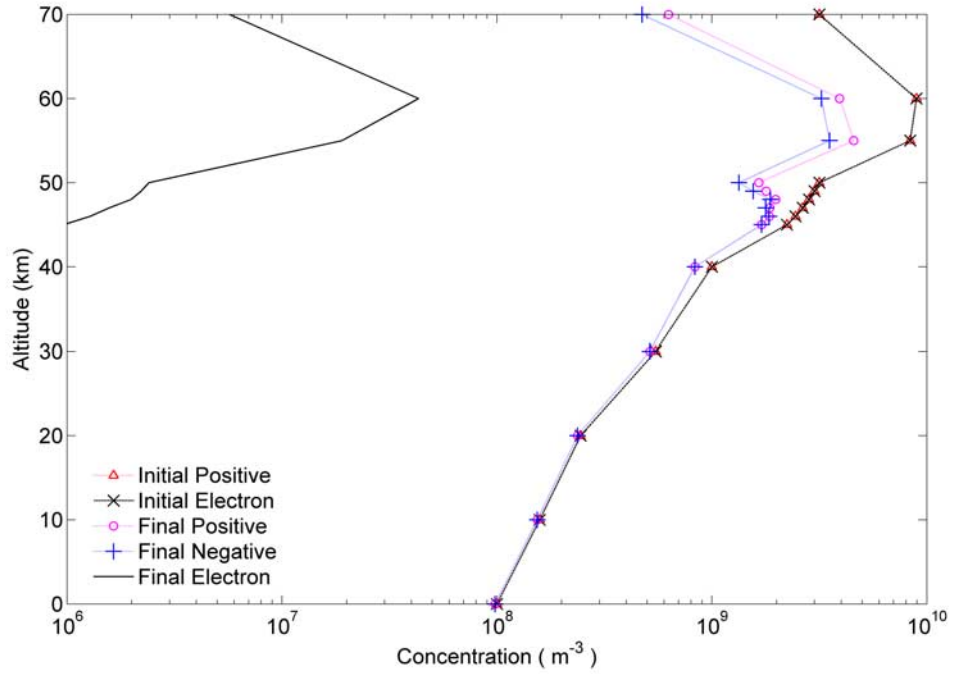


**Figure 17.** Initial and final concentration of ions and electrons when the distribution of particles is considered polydisperse.

using the monodisperse case. The effective attachment coefficients of the polydisperse distributed particles are found to be less by factors of 6 to 2 in the altitude region of 45 to 60 km compared to that of the monodisperse distributed particles. Though it is more convenient and computationally less expensive to use monodisperse distribution in the model, doing so overestimates the effect of cloud particles on atmospheric conductivity.

[29] *Rossow* [1978] calculated the time constants for the cloud microphysical processes in the atmospheres of Earth, Venus, Mars and Jupiter. *Carlson et al.* [1988] used the same method to calculate the time constants of predominant cloud microphysical processes in the atmospheres of giant planets. The time constants for coagulation (>$10^4$ s), evaporation (>$10^5$ s), sedimentation (>$10^3$ s) [*Rossow*, 1978], are found to be greater than the time required for the charging to

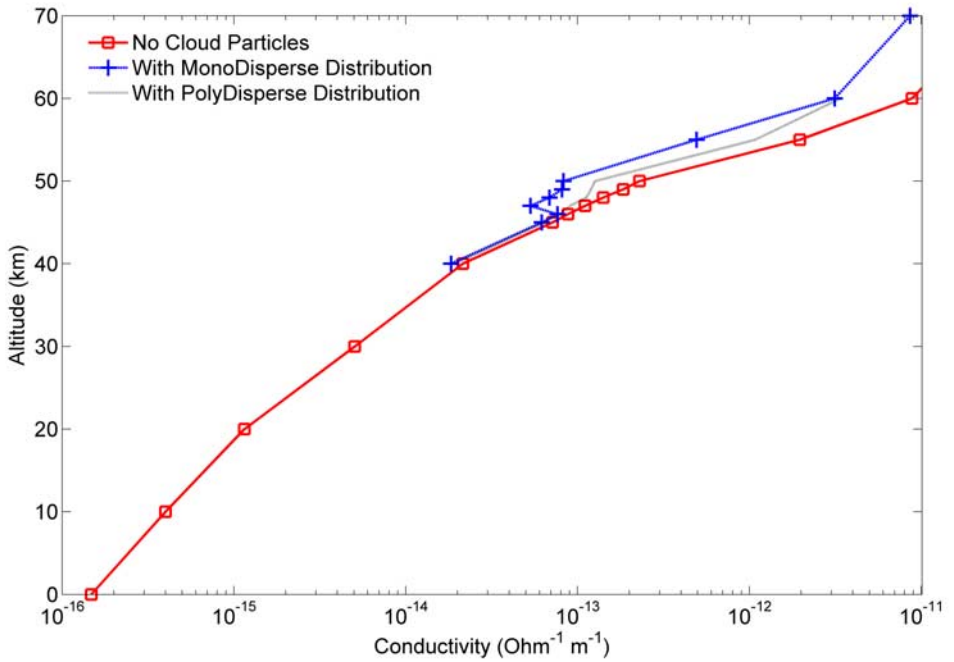


**Figure 18.** Altitude profile of conductivity for various conditions in the atmosphere of Venus.

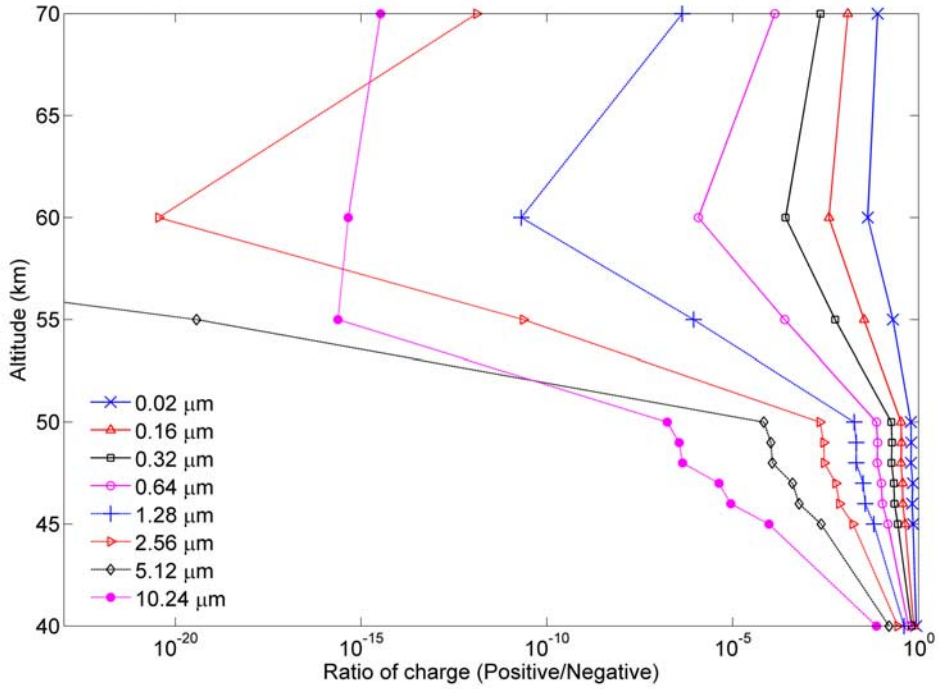


**Figure 19.** Ratio of total positive to negative charges accumulated on the cloud particles.

reach the steady state (<$10^3$ s). *Pruppacher and Klett* [1997] estimated the time constant for cloud droplet charging by ion diffusion close to the surface of the Earth as 400 s. Therefore the results presented would not be affected by the assumption of the same shape of the size distribution throughout the charging calculation.

### 5.3. Implications for Lightning in the Atmosphere

[30] *Russell et al.* [2007] observed signals which appear to be due to the lightning from the clouds using a magnetometer onboard Venus Express spacecraft. The signals obtained occurred in bursts, with rapidly varying amplitudes, and variable interburst spacings and durations. *Russell et al.* [2007] reported observations of strong circularly polarized electromagnetic waves which appear as bursts of radiation lasting 0.25 to 0.5 s and have the expected properties of whistler mode signals generated by lightning discharges in the clouds of Venus. The waveforms indicate an impulsive current source similar to terrestrial lightning and also, the intermittent appearance of the bursts is like the occurrence pattern expected from a weather-associated phenomenon [*Russell et al.*, 2007].

[31] Figure 19 presents the ratio of positive to negative charges acquired by the droplets of different sizes. It can be seen that in the lower cloud region the charge ratio is similar for particles of size less than 0.06 $\mu$m, whereas the ratio becomes much larger for larger particles in the middle and upper cloud regions. This suggests that there are more negatively charged particles in the middle and upper cloud region compared to the lower cloud region. As mentioned earlier, generation of more negatively charged particles at greater altitudes is due to the presence of larger concentration of highly mobile electrons, which get easily attached to particles, especially larger ones. It is clearly visible from Figure 19 that the ratio of the positive to negative charges shows a steep decrease for altitudes greater than 50 km and becomes saturated or changes direction for altitudes greater than 60 km. The occurrence of such a large charge separation is in agreement with the suggestion of *Russell et al.* [2006] that the middle cloud droplets can be charged like the cloud droplets on the terrestrial atmosphere where the temperature and pressure are similar. If vertical winds exist, then large particles can be physically separated from the small and an electric field will be generated. The electric field will build to the point where one of two situations occurs; either the electric current caused by the electric field limits the electric field to a value below the breakdown value, or the electric field exceeds that value and an electrical discharge occurs. An order of magnitude calculation given below shows that lightning discharges in the 40 to 70 km altitude range is highly unlikely.

[32] For the pressure range of interest, breakdown electric fields will be of the order $10^5$ to $10^6$ volts $m^{-1}$ [*Roussel-Dupré et al.*, 2008], which is similar to the terrestrial atmosphere. On the basis of the conductivities calculated (i.e., $\sim 10^{-13}$ ohm$^{-1}$ m$^{-1}$), the corresponding leakage currents would be $10^{-8}$ to $10^{-7}$ Am$^{-2}$. To reach the breakdown electric field, the charging current must exceed the leakage current. Even if the entire formation rate of electrons by GCR ($\sim 3 \times 10^7$ e s$^{-1}$ m$^{-3}$) went into charging the small aerosols and the vertical wind were just large enough (i.e., $2 \times 10^{-3}$ m s$^{-1}$) to levitate the small aerosols without levitating the large 4 $\mu$m radius particles, the charging current would be no larger than $10^{-14}$ Am$^{-2}$, many orders of magnitude too low to generate the electric field necessary for a lightning discharge. In the horizontal direction also, there is no obvious mechanisms to provide the work required to separate charges and, therefore, a lightning discharge is not expected.

[33] *Tzur and Levin* [1982] modeled the electric field near the surface of Venus by diffusion and conduction currents. It was found that a maximum of 30 $Vm^{-1}$ can be produced by diffusion at the surface and expected that if there is a charge separation within the cloud layers, it can affect the magnitude of the field [*Tzur and Levin*, 1982]. As the charging process studied here is more rapid than the particle-particle interaction and vertical transport, such a charge separation and development of electric field which can activate lightning seems unlikely in the atmosphere of Venus.

## 6. Conclusions

[34] Charging of cloud droplets in the atmosphere of Venus is examined in the present work. Charging occurs by the charge transfer by ions and attachment of electrons to the particles. GCR are the major source of ions and electrons in the altitudes of interest. Charge balance equations are constructed to estimate the steady state concentration of ions, electrons and particles which are charged as well as neutral. Both monodisperse and polydisperse distributions of particles were used and the results were compared. The present results compare favorably with those of *Borucki et al.* [1982] when the differences of aerosol properties are considered.

[35] The following are the major conclusions of the study: (1) Large number of charges are accumulated on particles in the altitude region 48 to 55 km because of the existence of larger sizes and greater concentration of particles. (2) Maximum reduction in ion concentration (at 50 km) was found to be a factor of 5 for monodisperse distribution of particles in the cloud layer, while *Borucki et al.* [1982] observed a maximum drop of an order of magnitude due to the higher surface area of the particles used in those calculations. (3) For polydisperse distribution of particles, the maximum reduction in ion concentration was found to be only a factor of 3, as the effective attachment coefficients of the polydisperse particles are lower than those of monodisperse distributed particles. (4) Therefore, monodisperse distribution overestimates the reduction in conductivity, though it is more convenient and computationally less expensive than the more realistic polydisperse distribution of particles. (5) Charging of aerosols by energetic particles and the separation of charge due to differential charging and vertical winds appears to be inadequate to generate the electric fields necessary to cause the lightning events some investigators have observed.

## References


Aplin, K. (2006), Atmospheric electrification in the solar system, *Surv. Geophys.*, *27*, 63–108, doi:10.1007/s10712-005-0642-9.

Arnold, H. R. (1964), Comments on a paper, "Collisional detachment and the formation of an ionospheric C region" by Pierce, E.T., *J. Res. Natl. Bur. Stand. U.S., Sect. D*, *68*, 215–217.

Bell, J. F., III, D. Crisp, P. G. Lucey, T. A. Ozorski, W. M. Sinton, S. C. Willis, and B. A. Campbell (1991), Spectroscopic observations of bright and dark emission features on the night side of Venus, *Science*, *252*, 1293–1296, doi:10.1126/science.252.5010.1293.

Bertaux, J. L., et al. (2007), SPICAV on Venus Express: Three spectrometers to study the global structure and composition of the Venus atmosphere, *Planet. Space Sci.*, *55*, 1673–1700, doi:10.1016/j.pss.2007.01.016.

Borucki, W. J., Z. Levin, R. C. Whitten, R. G. Keesee, L. A. Capone, O. B. Toon, and J. Dubach (1982), Predicted electrical conductivity between 0 and 80 km in the Venusian atmosphere, *Icarus*, *51*, 302–321, doi:10.1016/0019-1035(82)90086-0.

Borucki, W. J., J. W. Dyer, J. R. Phillips, and P. Pham (1991), Pioneer Venus orbiter search for Venusian lightning, *J. Geophys. Res.*, *96*, 11,033–11,043, doi:10.1029/91JA01097.

Borucki, W. J., R. C. Whitten, E. L. O. Bakes, E. Barth, and S. N. Tripathi (2006), Predictions of the electrical conductivity and charging of the aerosols in Titan's atmosphere 6/20/05, *Icarus*, *181*, 527–544, doi:10.1016/j.icarus.2005.10.030.

Carlson, B. E., W. B. Rossow, and G. S. Orton (1988), Cloud microphysics of giant planets, *J. Atmos. Sci.*, *45*, 2066–2081, doi:10.1175/1520-0469(1988)045<2066:CMOTGP>2.0.CO;2.

Carlson, R. W., L. W. Kamp, K. H. Baines, J. B. Pollack, D. H. Grinspoon, T. Encrenaz, P. Drossart, and F. W. Taylor (1993), Variations in Venus cloud particle properties: A new view of Venus's cloud morphology as observed by the Galileo near-infrared mapping spectrometer, *Planet. Space Sci.*, *41*, 477–485.

Chauzy, S., and S. Despieu (1980), Rainfall rate and electric charge and size of raindrops of six spring showers, *J. Atmos. Sci.*, *37*, 1619–1627, doi:10.1175/1520-0469(1980)037<1619:RRAECA>2.0.CO;2.

Chen, R. H., and A. F. Nagy (1978), A comprehensive model of the Venus ionosphere, *J. Geophys. Res.*, *83*, 1133–1140, doi:10.1029/JA083iA03p01133.

Christophorou, L. G. (1980), Negative ions of polyatomic molecules, *Environ. Health Perspect.*, *36*, 3–32, doi:10.2307/3429329.

Crisp, D., et al. (1989), The nature of the near-infrared features on the Venus night side, *Science*, *246*, 506–509, doi:10.1126/science.246.4929.506.

Crisp, D., et al. (1991), Ground-based near-infrared imaging observations of Venus during the Galileo encounter, *Science*, *253*, 1538–1541, doi:10.1126/science.253.5027.1538.

Desch, S. J., W. J. Borucki, C. T. Russell, and A. Bar-Nun (2002), Progress in planetary lightning, *Rep. Prog. Phys.*, *65*, 955–997, doi:10.1088/0034-4885/65/6/202.

Esposito, L. W., R. G. Knollenberg, M. Y. Marov, O. B. Toon, and R. P. Turco (1983), The clouds and hazes of Venus, in *Venus*, edited by D. M. Hunten et al., pp. 484–564, Univ. of Ariz. Press, Tucson.

Grinspoon, D. H., J. B. Pollack, B. R. Sitton, R. W. Carlson, L. W. Kamp, K. H. Baines, T. Encrenaz, and F. W. Taylor (1993), Probing Venus's cloud structure with Galileo NIMS, *Planet. Space Sci.*, *41*, 515–542.

Gurnett, D. A., W. S. Kurth, A. Roux, R. Gendrin, C. F. Kennel, and S. J. Bolton (1991), Lightning and plasma wave observations from the Galileo flyby of Venus, *Science*, *253*, 1522–1525, doi:10.1126/science.253.5027.1522.

Gurnett, D. A., P. Zarka, R. Manning, W. S. Kurth, G. B. Hospodarsky, T. F. Averkamp, M. L. Kaiser, and W. M. Farrell (2001), Non-detection at Venus of high-frequency radio signals characteristic of terrestrial lightning, *Nature*, *409*, 313–315, doi:10.1038/35053009.

Hansell, S. A., W. K. Wells, and D. M. Hunten (1995), Optical detection of lightning on Venus, *Icarus*, *117*, 345–351, doi:10.1006/icar.1995.1160.

Hansen, J. E., and J. W. Hovenier (1974), Interpretation of the polarization of Venus, *J. Atmos. Sci.*, *31*, 1137–1160, doi:10.1175/1520-0469(1974)031<1137:IOTPOV>2.0.CO;2.

Hoppel, W. A. (1985), Ion-aerosol attachment coefficients, ion depletion, and the charge distribution on aerosols, *J. Geophys. Res.*, *90*, 5917–5923, doi:10.1029/JD090iD04p05917.

Hoppel, W. A., and G. M. Frick (1986), Ion-aerosol attachment coefficients and the steady-state charge on aerosols in a bipolar ion environment, *Aerosol Sci. Technol.*, *5*, 1–21, doi:10.1080/02786828608959073.

Hua, H., and R. H. Holzworth (1996), Observations and parameterization of the stratospheric electrical conductivity, *J. Geophys. Res.*, *101*, 29,539–29,552, doi:10.1029/96JD01060.

Imamura, T., and G. L. Hashimoto (1998), Venus cloud formation in the meridional circulation, *J. Geophys. Res.*, *103*, 31,349–31,366, doi:10.1029/1998JE900010.

Imamura, T., and G. L. Hashimoto (2001), Microphysics of Venusian clouds in rising tropical air, *J. Atmos. Sci.*, *58*, 3597–3612, doi:10.1175/1520-0469(2001)058<3597:MOVCIR>2.0.CO;2.

James, E. P., O. B. Toon, and G. Schubert (1997), A numerical microphysical model of the condensational Venus cloud, *Icarus*, *129*, 147–171, doi:10.1006/icar.1997.5763.

Jensen, E. J., and G. E. Thomas (1991), Charging of mesospheric particles: Implications for electron density and particle coagulation, *J. Geophys. Res.*, *96*, 18,603–18,615, doi:10.1029/91JD01966.

Kawabata, K., D. L. Coffeen, J. E. Hansen, W. A. Lane, M. Sato, and L. D. Travis (1980), Cloud and haze properties from Pioneer Venus polarimetry, *J. Geophys. Res.*, *85*, 8129–8140, doi:10.1029/JA085iA13p08129.

Keesee, R. G., N. Lee, and A. W. Castleman Jr. (1980), Properties of clusters in the gas phase: V. Complexes of neutral molecules onto negative ions, *J. Chem. Phys.*, *73*, 2195–2202, doi:10.1063/1.440415.

Knollenberg, R. G., and D. M. Hunten (1980), The microphysics of the clouds of Venus: Results of the Pioneer Venus particle size spectrometer experiment, *J. Geophys. Res.*, *85*, 8039–8058, doi:10.1029/JA085iA13p08039.

Krasnopolsky, V. A. (1983), Lightning and nitric oxide on Venus, *Planet. Space Sci.*, *31*, 1363–1369, doi:10.1016/0032-0633(83)90072-7.

Krasnopolsky, V. A. (1989), Vega mission results and chemical composition of Venusian clouds, *Icarus*, *80*, 202–210, doi:10.1016/0019-1035(89)90168-1.

Krasnopolsky, V. A. (2007), Chemical kinetic model for the lower atmosphere of Venus, *Icarus*, *191*, 25–37, doi:10.1016/j.icarus.2007.04.028.

Krasnopolsky, V. A., and J. B. Pollack (1994), H2O-H2SO4 system in Venus' clouds and OCS, CO, and H2SO4 profiles in Venus' troposphere, *Icarus*, *109*, 58–78, doi:10.1006/icar.1994.1077.

Markiewicz, W. J., et al. (2007), Morphology and dynamics of the upper cloud layer of Venus, *Nature*, *450*, doi:10.1038/nature06320.

Michael, M., and S. N. Tripathi (2008), Effect of charging of aerosols in the lower atmosphere of mars during the dust storm of 2001, *Planet. Space Sci.*, *56*, 1696–1702, doi:10.1016/j.pss.2008.07.030.

Michael, M., M. Barani, and S. N. Tripathi (2007), Numerical predictions of aerosol charging and electrical conductivity of the lower atmosphere of Mars, *Geophys. Res. Lett.*, *34*, L04201, doi:10.1029/2006GL028434.

Michael, M., S. N. Tripathi, and S. K. Mishra (2008), Dust charging and electrical conductivity in the day and night-time atmosphere of Mars, *J. Geophys. Res.*, *113*, E07010, doi:10.1029/2007JE003047.

Mills, F. P., and M. Allen (2007), A review of selected issues concerning the chemistry in Venus' middle atmosphere, *Planet. Space Sci.*, *55*, 1729–1740, doi:10.1016/j.pss.2007.01.012.

O' Brien, K. (1970), Calculated cosmic ray ionization in the lower atmosphere, *J. Geophys. Res.*, *75*, 4357–4359, doi:10.1029/JA075i022p04357.

Parthasarathy, R. (1976), Mesopause dust as a sink for ionization, *J. Geophys. Res.*, *81*, 2392–2396.

Pollack, J. B., D. W. Strecker, F. C. Witteborn, E. F. Erickson, and B. J. Baldwin (1978), Properties of the clouds of Venus, as inferred from airborne observations of its near-infrared reflectivity spectrum, *Icarus*, *34*, 28–45.

Pollack, J. B., et al. (1993), Near infrared light from Venus' nightside: A spectroscopic analysis, *Icarus*, *103*, 1–42, doi:10.1006/icar.1993.1055.

Pruppacher, H. R., and J. D. Klett (1997), *Microphysics of Clouds and Precipitation*, 2nd ed., Kluwer Acad., Dordrecht, Netherlands.

Rossow, W. B. (1978), Cloud microphysics: Analysis of the clouds of Earth, Venus, Mars, and Jupiter, *Icarus*, *36*, 1–50, doi:10.1016/0019-1035(78)90072-6.

Roussel-Dupré, R., J. J. Colman, E. Symbalisty, D. Sentman, and V. P. Pasko (2008), Physical processes related to discharges in planetary atmospheres, *Space Sci. Rev.*, *137*, 51–82, doi:10.1007/s11214-008-9385-5.

Russell, C. T. (1991), Venus lightning, *Space Sci. Rev.*, *55*, 317–356.

Russell, C. T., R. J. Strangeway, and T. L. Zhang (2006), Lightning detection on the Venus Express mission, *Planet. Space Sci.*, *54*, 1344–1351, doi:10.1016/j.pss.2006.04.026.

Russell, C. T., T. L. Zhang, M. Delva, W. Magnes, R. J. Strangeway, and H. Y. Wei (2007), Lightning on Venus inferred from whistler-mode waves in the ionosphere, *Nature*, *450*, 661–662, doi:10.1038/nature05930.

Sagdeev, R. Z., et al. (1986), Overview of VEGA Venus balloon in situ meteorological measurements, *Science*, *231*, 1411–1414, doi:10.1126/science.231.4744.1411.

Taylor, F. W., et al. (1980), Structure and meteorology of the middle atmosphere of Venus: Infrared remote sensing from the Pioneer orbiter, *J. Geophys. Res.*, *85*, 7963–8006, doi:10.1029/JA085iA13p07963.

Tinsley, B. A., and L. Zhou (2006), Initial results of a global circuit model with variable stratospheric and tropospheric aerosols, *J. Geophys. Res.*, *111*, D16205, doi:10.1029/2005JD006988.

Toon, O. B., R. P. Turco, and J. B. Pollack (1982), The ultraviolet absorber on Venus: Amorphous sulfur, *Icarus*, *51*, 358–373, doi:10.1016/0019-1035(82)90089-6.

Tripathi, S. N., and M. Michael (2008), Aerosols in the atmosphere of Mars, in *Modeling of Planetary Atmosphere*, edited by S. A. Haider et al., chap. 3, Macmillan, India, in press.

Tripathi, S. N., M. Michael, and R. G. Harrison (2008), Profiles of ion and aerosol interactions in planetary atmospheres, *Space Sci. Rev.*, *137*, 193–211, doi:10.1007/s11214-008-9367-7.

Turco, R. P., O. B. Toon, R. C. Whitten, and R. G. Keesee (1983), Venus: Mesospheric hazes of ice, dust, and acid aerosols, *Icarus*, *53*, 18–25, doi:10.1016/0019-1035(83)90017-9.

Tzur, I., and Z. Levin (1982), A one-dimensional model of the atmospheric electric field near the Venusian surface, *Icarus*, *52*, 346–353, doi:10.1016/0019-1035(82)90117-8.

Upadhyay, H. O., R. R. Singh, and R. N. Singh (1994), Cosmic ray ionization of lower Venus atmosphere, *Earth Moon Planets*, *65*, 89–94, doi:10.1007/BF00572202.

Whitten, R. C., W. J. Borucki, and S. N. Tripathi (2007), Predictions of the electrical conductivity and charging of the aerosols in Titan's nighttime atmosphere, *J. Geophys. Res.*, *112*, E04001, doi:10.1029/2006JE002788.

Whitten, R. C., W. J. Borucki, and S. N. Tripathi (2008), Predictions of the electrical conductivity and charging of the cloud particles in Jupiter's atmosphere, *J. Geophys. Res.*, *113*, E04001, doi:10.1029/2007JE002975.

Yair, Y., and Z. Levin (1989), Charging of polydispersed aerosol particles by attachment of atmospheric ions, *J. Geophys. Res.*, *94*, 13,085–13,091, doi:10.1029/JD094iD11p13085.

Yair, Y., G. Fischer, F. Simões, N. Renno, and P. Zarka (2008), Updated review of planetary atmospheric electricity, *Space Sci. Rev.*, *137*, 29–49, doi:10.1007/s11214-008-9349-9.

Yamamoto, M., and M. Takahashi (2006), An aerosol transport model based on a two-moment microphysical parameterization in the Venus middle atmosphere: Model description and preliminary experiments, *J. Geophys. Res.*, *111*, E08002, doi:10.1029/2006JE002688.

Young, A. T. (1973), Are the clouds of Venus sulfuric acid?, *Icarus*, *18*, 564–582, doi:10.1016/0019-1035(73)90059-6.

W. J. Borucki, NASA Ames Research Center, Moffett Field, CA 94035, USA.

M. Michael and S. N. Tripathi, Department of Civil Engineering, Indian Institute of Technology, Kanpur 208016, India. (snt@iitk.ac.in)

R. C. Whitten, SETI Research Institute, 515 N. Whisman Road, Mountain View, CA 94043, USA.